J. Fluid Mech. (2003), *vol.* 480, *pp.* 25–42. © 2003 Cambridge University Press
DOI: 10.1017/S0022112002003294 Printed in the United Kingdom

Closed-form linear stability conditions for rotating Rayleigh–Bénard convection with rigid stress-free upper and lower boundaries

By R. C. KLOOSTERZIEL[1] AND G. F. CARNEVALE[2]

[1]School of Ocean and Earth Science and Technology, University of Hawaii, Honolulu, HI 96822, USA

[2]Scripps Institution of Oceanography, University of California, San Diego, La Jolla, CA 92093, USA

(Received 24 May 2002 and in revised form 9 September 2002)

The linear dynamics of rotating Rayleigh–Bénard convection with rigid stress-free boundaries has been thoroughly investigated by Chandrasekhar (1961) who determined the marginal stability boundary and critical horizontal wavenumbers for the onset of convection and overstability as a function of the Taylor number T. No closed-form formulae appeared to exist and the results were tabulated numerically. However, by taking the Rayleigh number R as independent variable we have found remarkably simple expressions. When the Prandtl number $P \geqslant P_c = 0.67659$, the marginal stability boundary is described by the curve $T(R) = R[(R/R_c)^{1/2} - 1]$ where $R_c = \frac{27}{4}\pi^4$ is Rayleigh's famous critical value for the onset of stationary convection in a non-rotating system ($T = 0$). For $P < P_c$ the marginal stability boundary is determined by this curve until it is intersected by the curve

$$T(R, P) = R\left[\left(\frac{1+P}{2^3 P^4}\right)^{1/2}(R/R_c)^{1/2} - \frac{1+P}{2P^2}\right].$$

A simple expression for the intersection point is derived and also for the critical horizontal wavenumbers for which, along the marginal stability boundary, instability sets in either as stationary convection or in an oscillatory fashion. A simple formula is derived for the frequency of the oscillations. Further, we have analytically determined critical points on the marginal stability boundary above which an increase of either viscosity or diffusivity is destabilizing. Finally, we show that if the fluid has zero viscosity the system is always unstable, in contradiction to Chandrasekhar's conclusion.

1. Introduction

Rayleigh–Bénard convection was first investigated theoretically by Rayleigh (1916) who was inspired by the experimental work of Bénard (1900) and the more qualitative work of Thomson (1882). A century before that, Rumford (1797) performed systematic experiments with convection in fluids heated from below. His work was inspired by an accident involving rice soup which was cold near the top but unfortunately still hot near the bottom of the bowl. He also wondered why dishes such as apple pies remain hot for remarkably long periods. The additional effect of rotation was first considered theoretically by Chandrasekhar (1953) and Chandrasekhar & Elbert (1955). The contents of these papers, with some modifications and additions, are in Chandrasekhar (1961) monograph (chapter III). Strictly speaking they studied

the influence of Coriolis forces in the dynamics and disregarded effects like curvature of iso-density surfaces as would occur in a rotating container, i.e. centrifugal forces are ignored. Here, we revisit this classical rotating linear RB-problem with stress-free rigid upper and lower boundaries. The top and bottom are considered perfect heat conductors, maintained at constant (different) temperatures, with the higher temperature at the bottom. The horizontal domain is unbounded, the Boussinesq approximation is made, incompressibility is assumed and the kinematic viscosity and diffusivity are constant. In § 2.1, we discuss the general properties of the cubic polynomial which determines the eigenvalues p for normal-mode perturbations with an assumed time dependence $\exp(pt)$. Almost an ancient subject now, we would expect that nothing new could be added to the literature, but we show in § 2.2 that the linear stability results tabulated in Chandrasekhar (1961, chap. 3) for this 'easy' case of so-called free–free boundaries in the vertical can be summarized concisely with simple closed-form formulae which hitherto appear not to have been noted. The marginal stability boundary is discussed in some detail since we had difficulty following Chandrasekhar's development in some places. In § 2.3, we show that in the limit of vanishing viscosity, Chandrasekhar's conclusions were wrong. In § 3, we discuss what happens if either viscosity or diffusivity is increased. We find that there are critical Taylor and Rayleigh numbers above which marginally stable systems are destabilized by an increase in either viscosity or diffusivity alone with all else held fixed. In § 4, we summarize the results and discuss some additional matters of possible interest.

2. Linear stability

In the standard RB-problem, density variations are caused by temperature variations. In the unperturbed system, the temperature distribution between the bottom at $z = 0$ and top at $z = d$, with z the vertical coordinate, is linear: $\bar{\mathscr{T}}(z) = \mathscr{T}_0 - \beta z$. The system rotates with an angular velocity Ω about the z-axis, which coincides with the direction of the acceleration due to gravity g, and, in the co-rotating frame of reference, the velocity field is zero. With β positive (an 'adverse' temperature gradient), the temperature at the bottom is higher than at the top. Density is assumed to vary with temperature $\mathscr{T}$ according to $\rho = \rho_0[1 + \alpha(\mathscr{T}_0 - \mathscr{T})]$ where $\mathscr{T}_0$ is a reference temperature (here the temperature at the bottom) for which $\rho = \rho_0$ and α the coefficient of volume expansion, assumed constant. The derivation of the equations governing the RB-problem for an incompressible fluid under the Boussinesq approximation and additional simplifying assumptions and their justification are extensively discussed by Chandrasekhar (1961) and, for example, Drazin & Reid (1981) or Manneville (1990) (for the non-rotating case). Linearizing the resulting equations about the basic motionless state, a set of coupled linear equations is derived for the evolution of small-amplitude velocity and temperature perturbations. The stability of the system is investigated by introducing velocity perturbations with a vertical component $w \propto \exp[pt + \mathrm{i}(k_x x + k_y y)] \sin(n\pi z/d)$ and horizontal components that vary instead with $\cos(n\pi z/d)$ plus temperature perturbations proportional to $\exp[pt + \mathrm{i}(k_x x + k_y y)] \sin(n\pi z/d)$. The vertical wavenumber takes the values $n = 1, 2, \cdots$. Chandrasekhar showed that the boundary conditions at the top and the bottom mentioned in § 1 will all be satisfied when the system is subjected to such perturbations and that stability/instability is determined by a cubic polynomial with the exponential time factor p as variable and coefficients that are functions of $k_x, k_y, n, d, \Omega, g\alpha\beta$ plus κ, the coefficient of thermal diffusivity and ν, the kinematic

viscosity. The cubic is (equations 239–240 in Chandrasekhar 1961, chap. 3, § 29)

$$\tilde{p}^3 + B\tilde{p}^2 + C\tilde{p} + D = 0 \quad \text{where} \quad \tilde{p} = (d^2/\nu)p, \tag{2.1}$$

and

$$\begin{aligned} B &= \frac{1+2P}{P}(a^2 + n^2\pi^2), \\ C &= \frac{1}{P}\left[(2+P)(a^2+n^2\pi^2)^2 + \frac{PTn^2\pi^2 - Ra^2}{a^2+n^2\pi^2}\right], \\ D &= \frac{1}{P}\left[(a^2+n^2\pi^2)^3 + Tn^2\pi^2 - Ra^2\right]. \end{aligned} \tag{2.2}$$

$$R = \frac{g\alpha\beta d^4}{\kappa\nu}, \quad T = \frac{(2\Omega)^2 d^4}{\nu^2}, \quad P = \frac{\nu}{\kappa}, \tag{2.3}$$

are the Rayleigh number, Taylor number and Prandtl number, respectively, and

$$a = |\boldsymbol{k}_{\mathrm{h}}|d = \left(k_x^2 + k_y^2\right)^{1/2} d$$

is the non-dimensional horizontal wavenumber. Note that p has been non-dimensionalized with the time scale d^2/ν which is what Chandrasekhar chose.

R, T and P characterize the system, and a and n the perturbations. If for given $\{R, T, P\}$ for all perturbations, the three roots of (2.1) have Re $p < 0$ there is stability. When, for certain perturbations, there is at least one root with Re $p > 0$, then there is instability. With each root of the cubic there is an associated combination of a flow field and temperature distribution, which we refer to as 'modes' although not explicitly considered here. The surface in the space spanned by $\{R, T, P\}$ separating stable systems from unstable systems defines the marginally stable states. As fully explained by Chandrasekhar (1961), when crossing from the stable to the unstable side, instability can set in as stationary convection in which case one root of (2.1) is $p = 0$, or in an oscillatory fashion when there are two purely imaginary, complex conjugate roots. The latter case is in some places referred to by Chandrasekhar as a case of overstability, whereas in other places overstability means cases of complex conjugate roots with Im $p \neq 0$ and Re $p > 0$, i.e. instability in the form of oscillations of increasing amplitude. We will, in what follows, also say that there is overstability when Im $p \neq 0$ while Re $p = 0$ and call the associated modes 'overstable modes'. We refer to associated with $p = 0$ as 'convective modes'.

2.1. *The eigenvalues*

The marginal stability boundary in the parameter space spanned by $\{R, T, P\}$ can be determined by examination of the coefficients B, C and D without actually solving the cubic. First, note that B in (2.2) is always positive. Since the coefficients are real, either the three roots are real or one root is real and the two other roots are complex conjugates. Graphically, the location of the real roots of the cubic can be found by looking for the intersection point of the curve

$$y = f(\tilde{p}) = \tilde{p}^3 + B\tilde{p}^2 + C\tilde{p}, \tag{2.4}$$

with the horizontal line $y = -D$. At the origin in the $y\tilde{p}$-plane, the slope of the curve is $\mathrm{d}_{\tilde{p}} f(\tilde{p})|_{\tilde{p}=0} = C$, and the curvature is equal to $2B$ which is always positive. Thus, for $C > 0$ it is upwards and for $C < 0$ downwards. When $C = 0$, the second derivative of f is $2B > 0$ and there is positive curvature at the origin while the curve has a horizontal tangent there.

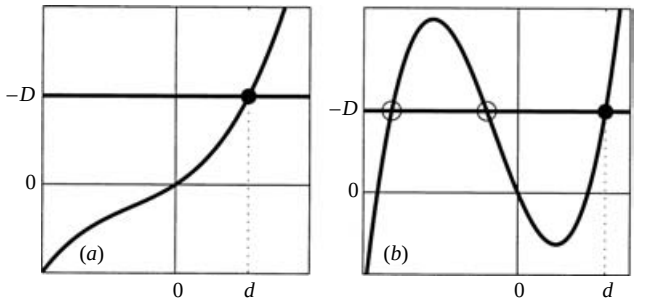

FIGURE 1. Graphs showing examples of the function (2.4) (solid curve) with $B > 0$ and the horizontal line $y = -D$ for $D < 0$. Intersections of the curve with the horizontal line determine the real roots of (2.1). There is either (*a*) one positive real root $\tilde{p} = d$, marked by ●, and the two other roots are complex conjugates or (*b*) the two other roots, marked by ○, are negative real. In either case, the real part of the two roots in addition to $\tilde{p} = d$ is negative (see text).

2.1.1. $D < 0$

When $D < 0$ there will be a positive real root $\tilde{p} = d$ of $f(\tilde{p}) = -D = |D|$ because the curve $f(\tilde{p})$ passes through the origin and then must cut the level line $y = |D| > 0$ as $\tilde{p}$ increases, since $f(\tilde{p}) \to +\infty$ for $\tilde{p} \to +\infty$. There may be a single real root, as in figure 1(*a*), or three real roots as in figure 1(*b*). If there are two additional real roots, they must be negative as can be seen geometrically from the condition that the curvature is positive at the origin since $B > 0$. If the additional roots are not real, they must be complex conjugates. In either case, we can prove that the two additional roots must have negative real parts. When the additional roots are real, say $\tilde{p} = b_1, b_2$ the cubic must equal $(\tilde{p} - b_1)(\tilde{p} - b_2)(\tilde{p} - d) = 0$ or

$$\tilde{p}^3 - (d + b_1 + b_2)\tilde{p}^2 + (b_1 b_2 + (b_1 + b_2)d)\tilde{p} - b_1 b_2 d = 0, \tag{2.5}$$

whereas if they are complex conjugates, say $\tilde{p} = b \pm \mathrm{i}\omega$, the cubic is

$$\tilde{p}^3 - (d + 2b)\tilde{p}^2 + (b^2 + \omega^2 + 2bd)\tilde{p} - (b^2 + \omega^2)d = 0. \tag{2.6}$$

Assuming real roots, (2.5) implies $b_1 b_2 > 0$ since $D = -b_1 b_2 d < 0$ and $d > 0$. Therefore, b_1 and b_2 have the same sign and are non-zero. Furthermore, we always have $B = -d - (b_1 + b_2) > 0$ and therefore $b_1 < 0$ and $b_2 < 0$, as sketched in figure 1(*b*). With (2.6), it follows that when the roots are complex conjugates, the real part $b < 0$ because $B = -d - 2b > 0$. In either case, therefore, there is one positive real root $\tilde{p} = d$ plus two roots with $\mathrm{Re}\ \tilde{p} < 0$.

2.1.2. $D > 0$

When $D > 0$ there will be one negative real root $\tilde{p} = -d$ of $f(\tilde{p}) = -D$ where the curve $f(\tilde{p})$ cuts the level line $y = -|D| < 0$, because the curve $f(\tilde{p})$ passes through the origin and $f(\tilde{p}) \to -\infty$ for $\tilde{p} \to -\infty$. Again, there could be a single real root as in figure 2(*a*), so that the other two roots are complex conjugates, or three real roots, as in figure 2(*b*, *c*). If the two additional roots are real the cubic must equal

$$\tilde{p}^3 + (d - (b_1 + b_2))\tilde{p}^2 + (b_1 b_2 - (b_1 + b_2)d)\tilde{p} + b_1 b_2 d = 0. \tag{2.7}$$

When the additional roots are complex conjugate roots the cubic is

$$\tilde{p}^3 + (d - 2b)\tilde{p}^2 + (b^2 + \omega^2 - 2bd)\tilde{p} + (b^2 + \omega^2)d = 0. \tag{2.8}$$

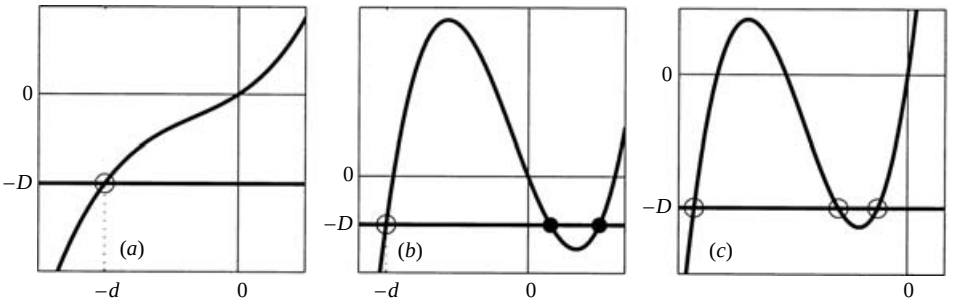

FIGURE 2. Graphs showing examples of the function (2.4) (solid curve) with $B > 0$ and the horizontal line $y = -D$ for $D > 0$. Intersections of the curve with the horizontal line determine the real roots of (2.1). There is either (*a*) one negative real root $\tilde{p} = -d$, marked by ○ and the two other roots are complex conjugates or (*b*) when $BC - D < 0$ the two other roots, marked by ●, are positive real and when (*c*) $BC - D > 0$ negative real. When there is one negative real root only, as in (*a*), the two other roots have Re $\tilde{p} > 0$ when $BC - D < 0$ and Re $\tilde{p} < 0$ when $BC - D > 0$. When $BC - D = 0$, the two additional roots have Re $\tilde{p} = 0$ and are $\tilde{p} = \pm \mathrm{i} C^{1/2}$ (see text).

The fact that $B > 0$ is no longer sufficient to determine the sign of the real parts of the additional roots, but the discriminant $BC - D$ is of help. From (2.7) and $D = b_1 b_2 d > 0$, it follows that

$$BC - D = (b_1 + b_2)^2 d - (b_1 + b_2)(d^2 + b_1 b_2), \quad b_1 b_2 > 0. \tag{2.9}$$

From (2.8), it follows that

$$BC - D = 4b^2 d - 2b(d^2 + b^2 + \omega^2). \tag{2.10}$$

There are three cases to be considered.

(i) $BC - D < 0$. In (2.9), the first term on the right-hand side is positive, since b_1 and b_2 are non-zero and have the same sign. The second term must be negative in order to have $BC - D < 0$. Thus, the factor $b_1 + b_2$ in the second term must be positive, since $d^2 + b_1 b_2 > 0$. It follows that $b_1 > 0$ and $b_2 > 0$, as in figure 2(*b*). Similarly, for complex conjugate roots, (2.10) implies $b \neq 0$ when $BC - D < 0$. Thus, the first term is positive and since $BC - D < 0$, the second term must again be negative which implies $b > 0$. In either case there is one negative real root $\tilde{p} = -d$ plus two roots with Re $\tilde{p} > 0$.

(ii) $BC - D > 0$. In this case it is convenient to write (2.9) and (2.10) as

$$BC - D = -(b_1 + b_2)(d^2 + C), \quad b_1 b_2 > 0, \tag{2.11}$$

and

$$BC - D = -2b(d^2 + C), \tag{2.12}$$

which follows from substitution of C from (2.7) and (2.8) into (2.9) and (2.10), respectively. Since $D > 0$ and $BC - D > 0$, it follows that $C > 0$ because $B > 0$ and therefore $d^2 + C > 0$ in both (2.11) and (2.12). For real roots, b_1 and b_2 are non-zero and have the same sign and therefore, according to (2.11), $b_1 < 0$ and $b_2 < 0$, as in figure 2(*c*). For complex conjugate roots, (2.12) implies that $b \neq 0$ since $C > 0$ and because $BC - D > 0$ we must have $b < 0$. Thus, all roots have Re $\tilde{p} < 0$.

(iii) $BC - D = 0$. Assuming that in addition to $\tilde{p} = -d$ there are two real roots, (2.11) implies that $b_1 + b_2 = 0$ because $C > 0$ and $d^2 + C > 0$. However, this contradicts $b_1 b_2 > 0$ which follows from $D = b_1 b_2 d > 0$. Thus, the additional roots cannot be real

	$D<0$	$D>0$	$D=0$
$BC-D<0$	Unstable	Unstable	Unstable
$BC-D>0$	Unstable	Stable	$\tilde{p}=0$ Re $\tilde{p}_+<0$ Re $\tilde{p}_-<0$
$BC-D=0$	Unstable	$\tilde{p}=-d$ $\tilde{p}_+=+\mathrm{i}\omega$ $\tilde{p}_-=-\mathrm{i}\omega$	$\tilde{p}=0$ $\tilde{p}_+=0$ $\tilde{p}_-<0$

TABLE 1. A summary of the properties of the roots of the cubic (2.1) when $B>0$. 'Stable' means all three roots have Re $\tilde{p}<0$ whereas 'unstable' means that at least one root has Re $\tilde{p}>0$. In the first column the sign of $BC-D$ is irrelevant since instability follows from $D<0$ alone (see text and figure 1).

and must be complex conjugates. With (2.12), we see that the two complex conjugate roots are purely imaginary when $BC-D=0$, i.e. $b=0$ and $\tilde{p}=\pm\mathrm{i}\omega$. Setting $b=0$ in (2.8), we find that $d=B$ and $\omega^2=C$.

2.1.3. $D=0$

Only when $D=0$ is $\tilde{p}=0$ a root, in which case, the other two roots are given by $\tilde{p}=-(\frac{1}{2}B)\pm[(\frac{1}{2}B)^2-C]^{1/2}$. These roots have a negative real part when $C>0$, since $B>0$. When $C<0$, one of the roots has a positive real part. When $C=0$, there is an additional root $\tilde{p}_+=0$ and $\tilde{p}_-=-B$. These three cases can be considered to correspond to $BC-D>0$, $BC-D<0$ and $BC-D=0$, respectively. Table 1 summarizes all the above.

2.2. *Determination of the marginal stability boundary*

2.2.1. *The convection curve*

The stability of the system is determined by the sign of D and $BC-D$. Equation (2.2) shows that $D<0$ when, for given a, n and T, R is large enough. $D>0$ for small enough R and $D=0$ when

$$(x+n^2\pi^2)^3+Tn^2\pi^2-Rx=0 \quad \text{where} \quad x\equiv a^2. \tag{2.13}$$

For fixed T and n, this determines a curve

$$R=\frac{1}{x}\left[(x+n^2\pi^2)^3+Tn^2\pi^2\right] \tag{2.14}$$

in the Rx-plane. An example is shown in figure 3(a). For large enough R and given n and T there are two positive x (or a), indicated by x_l and x_r, between which $D<0$. This implies instability according to table 1. $D>0$ for all x when R is smaller than a critical value R_c. Equation (2.13) shows that R_c will increase with increasing rotation (increasing T). This is indicated in figure 3(b) where we have drawn the curve (2.14) along which $D=0$ for $T=0$ together with that for $T>0$, both for the same n-value. R_c also increases with increasing vertical wavenumber n. R_c is determined by the condition that (2.13) is satisfied for just one positive x-value, indicated by x_c in figure 3. Chandrasekhar (1961) determined the critical Rayleigh number R_c and critical horizontal wavenumber $a_c=(x_c)^{1/2}$ by solving $\partial_x R=0$, with $R(x)$ as in (2.14). This is equivalent to finding the lowest point on the curves shown in figure 3.

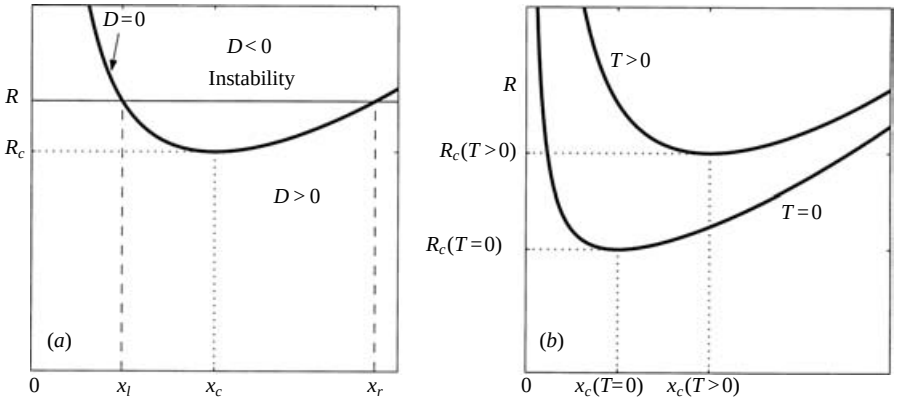

FIGURE 3. Graphs showing the curve (2.14) (thick line) as a function of $x = a^2$. (*a*) When $R > R_c$ the coefficient D in (2.1) is negative for $x_l < x < x_r$. This implies instability (see text and figure 1). When $R < R_c$, $D > 0$ for all x. The critical Rayleigh number R_c and corresponding critical wavenumber $a_c = x_c^{1/2}$ are where the curve has its minimum. (b) R_c and x_c or a_c increase with increasing rotation, measured by the Taylor number T. A similar increase occurs for increasing vertical wavenumber n (not shown).

$\partial_x R = 0$ when

$$2x^3 + 3n^2\pi^2x^2 = (n^2\pi^2)^3 + Tn^2\pi^2. \tag{2.15}$$

Chandrasekhar (1961) put $n = 1$ since this will yield the smallest critical Rayleigh number. He numerically determined the positive real root of this cubic as a function of T. This gives the critical horizontal wavenumber $a_c^{(c)}(T)$. Substituting this back into (2.14), he obtained the critical Rayleigh number $R_c^{(c)}(T)$. The superscript (c) indicates that these are critical values for convective modes, i.e. modes for which $\tilde{p} = 0$. This is how table VII of critical Rayleigh numbers and wavenumbers in Chandrasekhar (1961, chap. III) was compiled for a range of T-values. In the RT-plane these numerical values can be used to draw the curves $R_c^{(c)}(T)$ and $a_c^{(c)}(T)$ (figures 21 and 22 in Chandrasekhar 1961, chap. III).

An alternative approach that makes analytical progress possible is the following. Consider (2.13) and note that for given n and T, the critical Rayleigh number $R_c^{(c)}$ and wavenumber $a_c^{(c)}$ are determined by the condition that the straight line Rx is tangent to the third-order curve $(x + n^2\pi^2)^3 + Tn^2\pi^2$ as shown in figure 4(*a*). This occurs when

$$R = 3(x + n^2\pi^2)^2. \tag{2.16}$$

If (2.16) is put into (2.13), we obtain Chandrasekhar's problem: the cubic (2.15) has to be solved. However, we can solve (2.16) for x, i.e.

$$x = a^2 = \left(\tfrac{1}{3}R\right)^{1/2} - n^2\pi^2. \tag{2.17}$$

We took the positive root because a^2 must be positive. Substituting (2.17) into (2.13), we find the critical Taylor number $T_c^{(c)}$ as a function of R and n:

$$T_c^{(c)}(R, n) = R\left[(R/R_c(n))^{1/2} - 1\right] \quad \text{where} \quad R_c(n) = \tfrac{27}{4}n^4\pi^4. \tag{2.18}$$

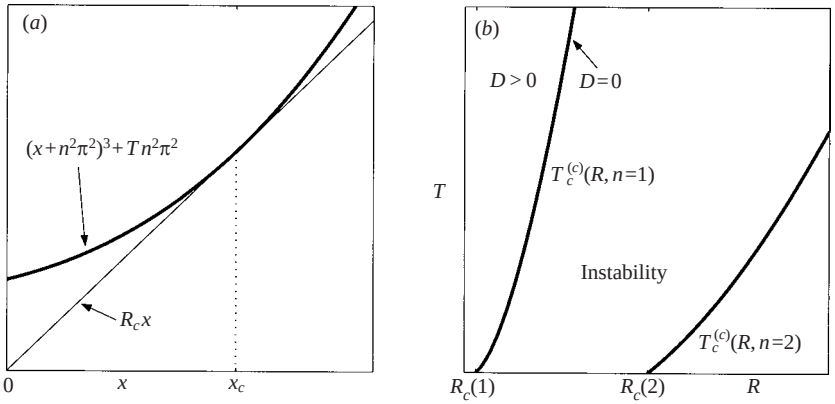

FIGURE 4. (*a*) The critical Rayleigh number R_c and corresponding wavenumber $a_c = x_c^{1/2}$ is found at the point where the straight line Rx is tangent to $(x+n^2\pi^2)^3 + Tn^2\pi^2$. (*b*) The critical Taylor number $T_c^{(c)}$ as a function of R for $n = 1$ and $n = 2$. The leftmost curve $T_c^{(c)}(R, n = 1)$, given by (2.19), starts on the R-axis at $R = R_c = \frac{27}{4}\pi^4$ and for $n > 1$ at $R = n^4 R_c$. For $\{R, T\}$ left of the curve $T_c^{(c)}(R, n = 1)$, $D > 0$ for all $\{a, n\}$. On the curve, $D = 0$ only when $\{a, n\} = \{a_c^{(c)}(R), 1\}$, with $a_c^{(c)}(R)$ given by (2.20), and $D > 0$ for all other $\{a, n\}$. For points $\{R, T\}$ to the right of the leftmost curve there are $\{a, n\}$ for which $D < 0$, implying instability, e.g. there will be a positive real root of (2.1).

In the RT-plane these curves start on the R-axis (where $T = 0$) at $R = R_c(n)$. The leftmost curve has $n = 1$, as shown in figure 4(*b*). It follows that $D > 0$ for all $\{a, n\}$ when $\{R, T\}$ is to the left of the curve

$$T_c^{(c)}(R) = R\left[(R/R_c)^{1/2} - 1\right] \quad \text{where} \quad R_c = R_c(n = 1) = \tfrac{27}{4}\pi^4 \approx 657.5. \tag{2.19}$$

This is the inverse of the (implicit) relation $R_c^{(c)}(T)$ numerically determined by Chandrasekhar (1961). When $\{R, T\}$ lies exactly on the curve (2.19), $D = 0$ for $\{a, n\} = \{a_c^{(c)}(R), 1\}$ with

$$a_c^{(c)}(R) = \left[\left(\tfrac{1}{3}R\right)^{1/2} - \pi^2\right]^{1/2}, \tag{2.20}$$

which follows from (2.17) with $n = 1$, but $D > 0$ for all other $\{a, n\}$. Thus, when $\{R, T\}$ lies on (2.19), there is one convective mode ($\tilde{p} = 0$) when $\{a, n\} = \{a_c^{(c)}(R), 1\}$ while for all other $\{a, n\}$ at least one mode is damped ($\tilde{p} < 0$; see figure 2). When $R = R_c$, $T_c^{(c)} = 0$ and $(\frac{1}{3}R)^{1/2} - \pi^2 = \frac{1}{2}\pi^2$ so that $a_c^{(c)}(R_c) = (\frac{1}{2}\pi^2)^{1/2}$. These are the critical Rayleigh and horizontal wavenumber found by Rayleigh (1916) for the non-rotating case. For $\{R, T\}$ to the right of the curve (2.19), there are a and n for which $D < 0$ and there will be unstable modes ($\tilde{p} > 0$; see figure 1).

As we have said, Chandrasekhar (1961) determined $a_c^{(c)}(T)$ and $R_c^{(c)}(T)$ numerically, but by switching to R as the independent variable rather simple closed-form formulae are found. When we compared the critical values that follow from our analytical expressions with those calculated by Chandrasekhar, we found that the errors in the latter were maximally 0.6% and in most cases much less than 0.1%. Such small errors can be considered round-off errors since Chandrasekhar's data were given to four significant digits.

2.2.2. *The overstability curve*

When $\{R, T\}$ lies to the left of the 'convection curve' (2.19), stability is not guaranteed. According to table 1, we have to investigate the sign of $BC - D$. It follows with (2.2) that

$$BC - D = 0 \quad \text{when} \quad (x + n^2\pi^2)^3 + \frac{P^2 T n^2 \pi^2}{(1+P)^2} - \frac{Rx}{2+2P} = 0. \tag{2.21}$$

Observing that (2.21) follows from (2.13) by replacing R with $R/(2+2P)$ and T with $P^2T/(1+P)^2$, we find that along the curve

$$T_c^{(o)}(R, P) = R\left[\left(\frac{1+P}{2^3P^4}\right)^{1/2}\left(\frac{R}{R_c}\right)^{1/2} - \frac{1+P}{2P^2}\right], \tag{2.22}$$

$BC - D = 0$ when $\{a, n\} = \{a_c^{(o)}(R, P), 1\}$ and

$$a_c^{(o)}(R, P) = \left[\left(\frac{R}{6+6P}\right)^{1/2} - \pi^2\right]^{1/2}. \tag{2.23}$$

For all other $\{a, n\}$, $BC - D > 0$ when $\{R, T\}$ lies on (2.22). When $\{R, T\}$ is to the left of (2.22), $BC - D > 0$ for all $\{a, n\}$ and when $\{R, T\}$ is to the right of (2.22), $BC - D < 0$ for some $\{a, n\}$. The curve $T_c^{(o)}(R, P)$ starts on the R-axis at $R = 2(1+P)R_c$. This follows from setting $T_c^{(o)} = 0$ in (2.22). For all $P \geqslant 0$, this is to the right of the starting point of the convection curve (2.19). The superscript (o) in (2.22) and (2.23) indicates that these are critical numbers for which there are overstable modes, as will be seen shortly. Since

$$(1+P)^{1/2}/(2^3P^4)^{1/2} = 1 \quad \text{for} \quad P = P_c \approx 0.67659, \tag{2.24}$$

the coefficient multiplying $R^{3/2}$ in (2.22) is smaller than unity when $P > P_c$. In that case, (2.22) stays to the right of the convection curve (2.19), as shown in figure 5(*a*). When $P < P_c$, (2.19) and (2.22) intersect at

$$R_i(P) = (1+\gamma)^2 R_c, \quad T_i(P) = \gamma(1+\gamma)^2 R_c, \quad \gamma = \frac{2^{1/2}(1+P) - (1+P)^{1/2}}{(1+P)^{1/2} - 2^{3/2}P^2}, \tag{2.25}$$

which is found by equating (2.19) to (2.22). When $P = P_c$, (2.22) asymptotically approaches (2.19) in the limit $R \to \infty$ and the intersection point is formally at infinity. In figures 5(*b*)–5(*d*), we show that, with decreasing $P < P_c$, the intersection point moves down. The lowest point in the RT-plane occurs in the limit $P \to 0$ for which $R_i = 2R_c$ and $T_i = 2(2^{1/2} - 1)R_c$. Chandrasekhar (1961) believed that there is no simple formula such as (2.25) for the intersection point. He calculated it numerically for several P-values. Comparison of his results with the exact values given by (2.25) revealed errors mostly of the order of 1% with one notable exception where it was almost 6%. Chandrasekhar used the transformation linking (2.21) to (2.13) to calculate the critical Rayleigh number $R_c^{(o)}$ and wavenumber $a_c^{(o)}$ as a function of T for $P = 0.025$ (the number for mercury) from the data in his table VII in chapter III. When we compared our theoretical values according to (2.22) and (2.23) for this case of $P = 0.025$ with his, errors were again found to be very small, i.e. roughly comparable to the round-off error due to tabulating the results only to the fourth significant digit.

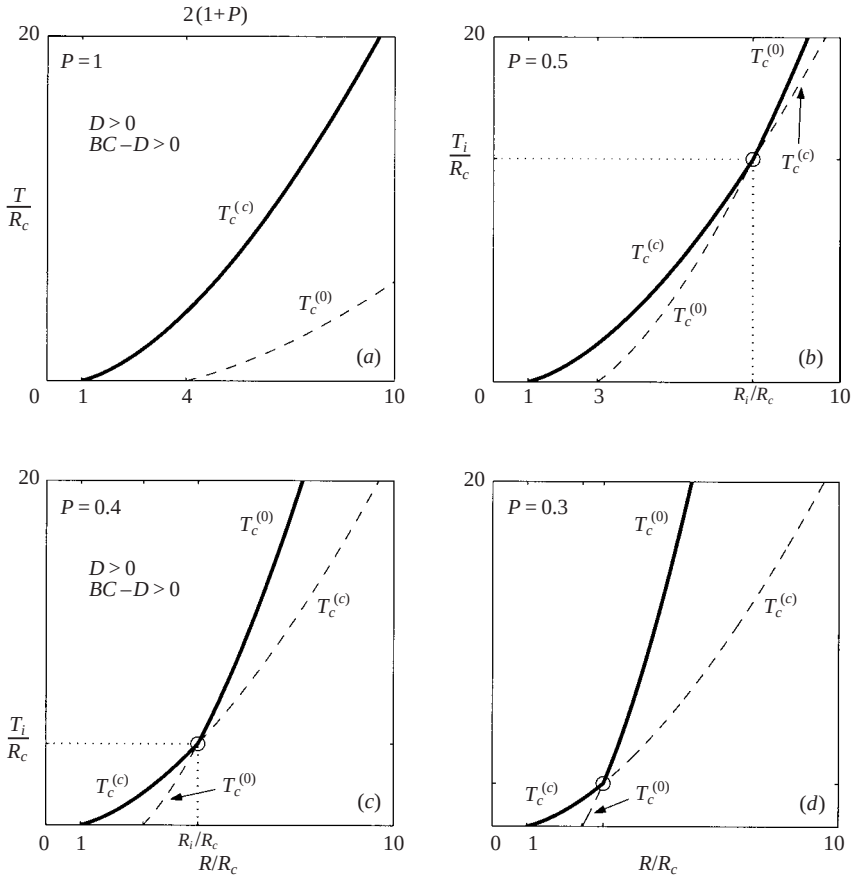

FIGURE 5. (*a*) Graph showing that when $P = 1$, the overstability curve $T_c^{(o)}(R, P)$ (2.22) does not cut the convection curve $T_c^{(c)}(R)$ (2.19). The overstability curve starts at $R = 2(1 + P)R_c$, the convection curve at $R = R_c$. This example with $P = 1$ is representative for all $P \geqslant P_c$. (*b*)–(*d*) For $P < P_c$, the curves cut at $\{R, T\} = \{R_i(P), T_i(P)\}$ (marked by ○). $R_i(P)$ and $T_i(P)$ are given by (2.25) and decrease with decreasing P. In the limit $P = 0$, $R_i = 2R_c$ and $T_i = 2(2^{1/2} - 1)R_c$, whereas for $P \to P_c$, $R_i, T_i \to \infty$.

2.2.3. *The marginal stability boundary*

When $P \geqslant P_c$, consider the 'boundary' consisting of the convection curve (2.19) drawn as a thick line in figure 5(*a*) and when $P < P_c$, the boundary composed of the convection curve (2.19) for $R_c \leqslant R \leqslant R_i$ and the 'overstability curve' (2.22) for $R > R_i$ (thick lines in figure 5*b–d*). For all points $\{R, T\}$ to the left of this boundary $D > 0$ and $BC - D > 0$ for perturbations with any $\{a, n\}$. According to table 1, the system is stable for such R and T values, i.e. the three roots of the cubic have $\mathrm{Re}\,\tilde{p} < 0$ for all $\{a, n\}$.

If $\{R, T\}$ is a point on the convection curve section $T_c^{(c)}(R)$ of the boundary, excluding the intersection point (if any), there will be one convective mode ($\tilde{p} = 0$) when $\{a, n\} = \{a_c^{(c)}(R), 1\}$, since then $D = 0$ and the other two modes are damped according to table 1 because $BC - D > 0$ for all $\{a, n\}$ on this section (recall that as discussed in § 2.2.2 $BC - D > 0$ to the left of the overstability curve). For all other $\{a, n\}$, each mode is damped according to table 1 because then both $D > 0$ and

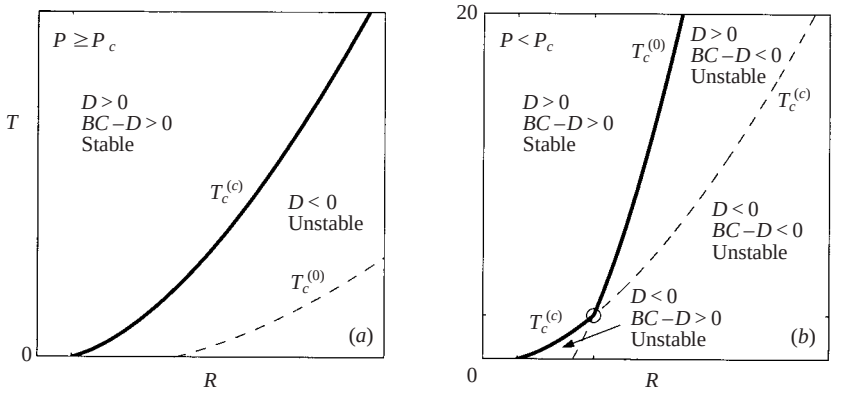

FIGURE 6. Graphs summarizing the stability properties of the system (*a*) for $P \geqslant P_c$ and (*b*) for $P < P_c$ where ○ indicates the intersection point $\{R_i, T_i\}$. Stability/instability as indicated follows from table 1.

$BC - D > 0$. When $\{R, T\}$ is on the overstability curve section $T_c^{(o)}(R, P)$, excluding the intersection point, all modes are damped for $\{a, n\} \neq \{a_c^{(o)}(R, P), 1\}$ because then $BC - D > 0$ while $D > 0$ for all $\{a, n\}$ on this section. $BC - D = 0$ when $\{a, n\} = \{a_c^{(o)}(R, P), 1\}$ and since $D > 0$ there is then one damped mode and two oscillatory or overstable modes (see table 1). The overstable modes are associated with the roots

$$\tilde{p}_{\pm} = \pm \mathrm{i}\omega \quad \text{where} \quad \omega^2 = C, \tag{2.26}$$

as shown in § 2.1.2. At the intersection point $\{R_i, T_i\}$ both $D > 0$ and $BC - D > 0$ except when $\{a, n\} = \{a_c^{(c)}(R), 1\}$ or $\{a, n\} = \{a_c^{(o)}(R, P), 1\}$. For all $\{a, n\}$, excluding these two cases, each mode is damped. When $\{a, n\} = \{a_c^{(o)}(R, P), 1\}$ there are two overstable modes and a damped mode since then $BC - D = 0$ and $D > 0$ because $a_c^{(o)}(R, P) \neq a_c^{(c)}(R)$ as is seen by comparing (2.20) and (2.23). When $\{a, n\} = \{a_c^{(c)}(R), 1\}$, there is a convective mode and two damped modes because then $BC - C > 0$ and $D = 0$. Thus, all along the boundary no roots have Re $\tilde{p} > 0$. If $\{R, T\}$ crosses the boundary to the right, we enter territory where either $D < 0$ or $BC - D < 0$ for some $\{a, n\}$ as indicated schematically in figure 6. Table 1 shows that there will be instability. This proves that, for $P \geqslant P_c$, the convection curve (2.19) is the marginal stability boundary (figure 6*a*) and for $P < P_c$, the curve composed of the convection curve (2.19) up to the intersection point $\{R_i, T_i\}$ and then continued by the overstability curve (2.22) (figure 6b).

The value of the non-dimensional oscillation frequency ω of the overstable modes is obtained by substituting $T = T_c^{(o)}(R, P)$, $n = 1$ and $a = a_c^{(o)}(R, P)$ in C which results in

$$\omega^2(R, P) = \frac{1 - P}{P^2} \left[\frac{\frac{1}{3} - \frac{1}{2}P^2}{1 - P^2} R - \left(\tfrac{3}{2}\right)^{1/2} (1 + P)^{1/2} \pi^2 R^{1/2} \right]. \tag{2.27}$$

Chandrasekhar (1961) derived that (he uses σ instead of ω)

$$\omega^2 = \frac{1 - P}{1 + P} \frac{T\pi^2}{a^2 + \pi^2} - (a^2 + \pi^2)^2, \tag{2.28}$$

which also yields (2.27) when $T = T_c^{(o)}(R, P)$ and $a = a_c^{(o)}(R, P)$ are substituted. Chandrasekhar (1961) used the transform noted into § 2.2.2 linking the results for the convection curve to that for the overstability curve to calculate the critical horizontal wavenumber for overstability as a function of T and P, i.e. $a_c^{(o)}(T, P)$. These values of $a_c^{(o)}(T, P)$ were substituted in (2.28). Comparison of our theoretical values (2.27) with those calculated by Chandrasekhar for a range of T-values and $P = 0.025$ (table XI in Chandrasekhar 1961, chap. III) revealed that the errors are negligibly small, again comparable to the round-off error (four significant digits).

2.3. *The limit* $\nu \to 0$

If we let $\nu \to 0$ with a non-zero fixed κ, we must be careful because R, T and the coefficients (2.2) become infinite. The singular behaviour of the cubic occurs because we chose the time scale d^2/ν to non-dimensionalize p. This does not occur if the cubic is written in its dimensional form, which is obtained by multiplying (2.1) with $(\nu/d^2)^3$. We then obtain $p^3 + B'p^2 + C'p + D' = 0$ where $B' = (\nu/d^2)B$, $C' = (\nu/d^2)^2 C$ and $D' = (\nu/d^2)^3 D$. Limits such as $\kappa \to 0$ and $\nu \to 0$ can safely be taken because B', C' and D' remain finite. Non-dimensionalizing with the finite time scale d^2/κ and letting $\nu \to 0$ we get

$$\tilde{p}^3 + (a^2 + n^2\pi^2)\tilde{p}^2 + \left[\frac{T'n^2\pi^2 - Ga^2}{a^2 + n^2\pi^2}\right]\tilde{p} + T'n^2\pi^2 = 0 \quad \text{with} \quad \tilde{p} = (d^2/\kappa)p. \tag{2.29}$$

The non-dimensional numbers are

$$T' = \frac{(2\Omega)^2 d^4}{\kappa^2}, \quad G = \frac{g\alpha\beta d^4}{\kappa^2}. \tag{2.30}$$

Identifying

$$D = T'n^2\pi^2, \quad BC - D = -Ga^2, \tag{2.31}$$

it follows from table 1, since $D > 0$ and $BC - D < 0$, that the system is always unstable (there is always a real negative root $\tilde{p} = -d$ and two roots with $\mathrm{Re}\ \tilde{p} > 0$). There are no convective modes ($\tilde{p} = 0$ is not a root because $D \neq 0$) and no purely oscillatory modes ($\tilde{p} = \pm i\omega$ are not roots because $BC - D \neq 0$). It is easy to show that also in the limit of zero diffusivity ($\lim \kappa \to 0$) the system is always unstable.

3. Destabilization due to increased viscosity or diffusivity

In the absence of rotation, stability is solely determined by the Rayleigh number and its value compared to the critical number R_c. If we consider a system characterized by some value $R = R_0$ close to R_c, it follows that an increase in viscosity or diffusion can decrease R to a value less than R_c and in that sense we call this 'stabilizing'. Similarly, a decrease in the adverse temperature gradient β or the vertical extent of the domain d is also stabilizing. In each case, these results are physically easily understood. In the rotating system, there are some surprises however.

First, consider the effect of changing viscosity. Let R_0 and T_0 be the Rayleigh and Taylor number for some initial viscosity ν_0, i.e.

$$R_0 = \frac{g\alpha\beta d^4}{\kappa\nu_0}, \quad T_0 = \frac{(2\Omega)^2 d^4}{\nu_0^2}. \tag{3.1}$$

With $R(\nu)$ and $T(\nu)$ the Rayleigh and Taylor number for variable ν and with all else held fixed, we have

$$T(\nu) = \frac{R^2(\nu)T_0}{R_0^2}, \quad \frac{\mathrm{d}T}{\mathrm{d}\nu} = \frac{2RT_0}{R_0^2}\frac{\mathrm{d}R}{\mathrm{d}\nu}. \tag{3.2}$$

Thus, the tangent to the curve traced out by $\{R(\nu), T(\nu)\}$ as ν varies is

$$\frac{\mathrm{d}T}{\mathrm{d}R} = \frac{2R(\nu)T_0}{R_0^2}. \tag{3.3}$$

If $\{R_0, T_0\}$ lies on the convection curve (2.19), the tangent there is

$$\left.\frac{\mathrm{d}T}{\mathrm{d}R}\right|_{R=R_0} = \frac{2T_0}{R_0} = 2\left(\frac{R_0}{R_c}\right)^{1/2} - 2, \tag{3.4}$$

which follows from (3.3) by setting $\nu = \nu_0$ and substituting $T_0 = T_c^{(c)}(R_0)$. The tangent to the convection curve at such a point $\{R_0, T_0\}$ is

$$\left.\frac{\mathrm{d}T_c^{(c)}(R)}{\mathrm{d}R}\right|_{R=R_0} = \tfrac{3}{2}(R_0/R_c)^{1/2} - 1. \tag{3.5}$$

Equating (3.4) to (3.5), we find that the tangents are equal at $\{R_0, T_0\} = \{R_c^\nu, T_c^\nu\}$ where

$$R_c^\nu = 4R_c, \quad T_c^\nu = 4R_c. \tag{3.6}$$

When the initial Prandtl number $P_0 = \nu_0/\kappa \geqslant P_c$, the stability boundary is the convection curve (figure 6*a*). An increase in ν increases P and the stability boundary therefore remains unchanged. For points on the convection curve (2.19) with $\{R_0, T_0\} < \{R_c^\nu, T_c^\nu\}$ an increase in viscosity, which decreases both R and T, puts us into the stable domain because (3.4) is smaller than (3.5) at such points. This is illustrated in figure 7(*a*) where we show the curve $\{R(\nu), T(\nu)\}$ when ν is doubled from ν_0 to $2\nu_0$, starting at a point below the critical point $\{R_c^\nu, T_c^\nu\}$. Clearly, after doubling the viscosity, the final point is on the stable side of the marginal stability boundary. For $\{R_0, T_0\} > \{R_c^\nu, T_c^\nu\}$, (3.4) is greater than (3.5) and an increase takes us into the unstable domain. This is illustrated in figure 7(*b*) where the final point is on the unstable side of the stability boundary after doubling the viscosity. Thus, for high-enough Rayleigh or Taylor numbers ($R > R_c^\nu = 4R_c \approx 2630$) an increase in viscosity is destabilizing. For any stable point off the stability curve, it is straightforward to calculate the increase in viscosity required to destabilize the system from the analytic expression for the curve.

When $0 < P_0 < P_c$, the marginal stability boundary is the convection curve (2.19) for $R_c \leqslant R \leqslant R_i$ and the overstability curve (2.22) for $R \geqslant R_i$ (figure 6*b*). A change in the viscosity ν changes P, and the stability boundary therefore changes simultaneously with the value of R and T. With (2.25), it follows that $\{R_i, T_i\} = \{R_c^\nu, T_c^\nu\}$ when $\gamma = 1$, which occurs for $P \approx 0.3192$. Therefore, for $P_0 < 0.3192$, all initial points on the convection curve section satisfy $\{R_0, T_0\} < \{R_c^\nu, T_c^\nu\}$ and an increase in viscosity is stabilizing as before since the intersection point (where the overstability curve section starts) moves up and to the right because P increases (see figure 5) while $\{R, T\}$ moves down and to the left into the stable domain as in figure 7(*a*). For $0.3192 < P_0 < P_c$,

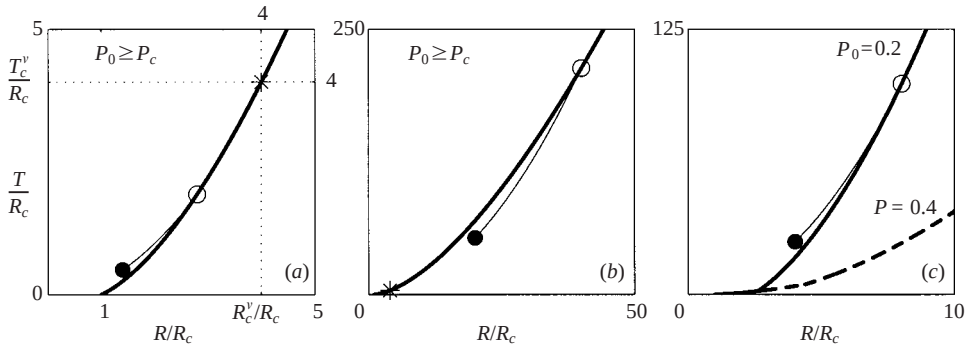

FIGURE 7. Graphs illustrating the stabilizing/destabilizing influence of increasing viscosity. Initial points $\{R_0, T_0\}$ for some initial viscosity ν_0 are marked by ○. In each case, the viscosity is increased to $2\nu_0$ and the final $\{R, T\}$ is marked by ●. (*a*) When $P_0 \geqslant P_c$, an increase in viscosity is stabilizing for points initially on the marginal stability boundary (thick line) when below the critical point $\{R_c^v, T_c^v\}$ (marked by $*$) but (*b*) destabilizing when above it. In these cases, the stability boundary is the convection curve (2.19). When $P_0 < P_c$ and the initial point lies on the overstability section of the marginal stability boundary, an increase is stabilizing. (*c*) This is illustrated with an example for $P_0 = 0.2$. After doubling the viscosity, the final point ● is to the left of the new stability boundary (dashed line) which in this example is for $P = 0.4$.

there are points on the convection curve section that lie above $\{R_c^v, T_c^v\}$ and for those an increase is destabilizing. For points $\{R_0, T_0\}$ on the overstability curve section some finite distance away from the intersection point, an increase in viscosity is stabilizing since $\{R, T\}$ moves down and to the left whereas the overstability curve section moves to the right, thus putting $\{R, T\}$ left of the shifted stability boundary. This is illustrated in figure 7(*c*).

A change in diffusivity alters the Rayleigh and Prandtl number but leaves the Taylor number unchanged. Let R_0 and P_0 be the Rayleigh and Prandtl number for some initial diffusivity κ_0, i.e.

$$R_0 = \frac{g\alpha\beta d^4}{\kappa_0 \nu}, \quad P_0 = \frac{\nu}{\kappa_0}.$$

If $R(\kappa)$ and $P(\kappa)$ denote the Rayleigh and Prandtl number for arbitrary κ we have

$$R(\kappa) = \frac{R_0}{P_0} P(\kappa), \quad \delta R = \frac{R_0}{P_0} \delta P, \tag{3.7}$$

where δR and δP are the changes due to a change $\delta\kappa$ of the diffusivity. Consider a point $\{R_0, T_0\}$ on the overstability curve section of the stability boundary, i.e. $\{R_0, T_0\}$ satisfies (2.22) with $P = P_0$ and $R_0 > R_i$. The shift of the overstability curve owing to a change δP is determined by substitution of $P = P_0 + \delta P$ in (2.22). If, for a given T_0, we indicate with R' the corresponding R-value on the overstability curve for $P = P_0 + \delta P$, then the horizontal distance between the original point $\{R_0, T_0\}$ and the new point $\{R', T_0\}$ is $|\delta R'| = |R' - R_0|$. If for increasing diffusivity ($\delta\kappa > 0$), which corresponds to negative δP, $|\delta R| < |\delta R'|$ then this is stabilizing, since then $R = R_0 - |\delta R|$ lies to the left of the shifted overstability curve, and stabilizing when $|\delta R| > |\delta R'|$. Using $T_c^{(o)}(R_0, P_0) = T_c^{(o)}(R_0 + \delta R', P_0 + \delta P)$ with $T_c^{(o)}(R, P)$ given by (2.22), a relation between $\delta R'$ and δP can be derived such that $\delta T_c^{(o)} = 0$. Expanding

the right-hand side of this equality in a double Taylor-series we find

$$\left[\left\{\frac{(1+P_0)^{1/2}}{2^{1/2}P_0}-\frac{1}{2^{5/2}(1+P_0)^{1/2}}\right\}\left(\frac{R_0^3}{R_c}\right)^{1/2}-\left(\frac{1}{2}+\frac{1}{P_0}\right)R_0\right]\delta P$$
$$=\left[\frac{3(1+P_0)^{1/2}}{2^{5/2}}\left(\frac{R_0}{R_c}\right)^{1/2}-\frac{1+P_0}{2}\right]\delta R'+O(\delta R'^2,\delta P^2,\delta R'\delta P). \quad (3.8)$$

Assuming that $\delta R'$ and δP are small, we find after some rearrangements that

$$\delta R'=\frac{\dfrac{3(1+P_0)^{1/2}}{2^{3/2}}\left(\dfrac{R_0}{R_c}\right)^{1/2}-(1+P_0)+\dfrac{(R_0/R_c)^{1/2}}{2^{3/2}(1+P_0)^{1/2}}-1}{\dfrac{3(1+P_0)^{1/2}}{2^{3/2}}\left(\dfrac{R_0}{R_c}\right)^{1/2}-(1+P_0)}\times\frac{R_0}{P_0}\delta P. \quad (3.9)$$

With (2.22), it follows that the term

$$\frac{3(1+P_0)^{1/2}}{2^{3/2}}\left(\frac{R_0}{R_c}\right)^{1/2}-(1+P_0)=3P_0^2\frac{T_0}{R_0}+\frac{1+P_0}{2},$$

is positive. Comparing (3.9) to (3.7), we see that if

$$\frac{(R_0/R_c)^{1/2}}{2^{3/2}(1+P_0)^{1/2}}\lesseqgtr 1 \quad \text{then} \quad |\delta R'|\lesseqgtr|\delta R|. \quad (3.10)$$

Equality occurs when (dropping the subscript 0)

$$R=8(1+P)R_c\equiv R_c^\kappa, \quad T=\frac{4(1+P)^2}{P^2}R_c\equiv T_c^\kappa. \quad (3.11)$$

R_c^κ follows from equality in (3.10) and T_c^κ subsequently by substitution of $R=R_c^\kappa$ in (2.22). For initial points $\{R, T\}$ on the overstability curve, therefore, a slight increase in diffusivity is stabilizing when $\{R_0, T_0\}<\{R_c^\kappa, T_c^\kappa\}$, but for $\{R_0, T_0\}>\{R_c^\kappa, T_c^\kappa\}$ an increase is destabilizing. Figure 8(*a*) illustrates this for the case $P_0=0.4$ and a change from κ_0 to $2\kappa_0$ so that the final Prandtl number is $P=0.2$. It is seen that in this example the point starting below $\{R_c^\kappa, T_c^\kappa\}$ ends up on the stable side of the new stability boundary. The point that starts above the critical point is, after doubling κ, on the unstable side of the new stability boundary. In figure 8(*b*) we show two more examples where the initial points lie farther up the overstability curve than in figure 8(*a*), and the destabilizing effect of doubling κ is seen more clearly.

When $P_0>P_c$ and $\{R_0, T_0\}$ lies on the convection curve (the stability boundary for $P\geqslant P_c$), a small increase in κ not exceeding some threshold so that P remains greater than P_c, lowers R and takes us into the stable domain since the boundary is unchanged. Cases where $P_0\leqslant P_c$ or the increase in κ is such that P becomes smaller than P_c are difficult to analyse mathematically. We find, generally, that if an initial point $\{R_0, T_0\}$ lies on the convection curve section of the stability boundary, for increased κ, the new point $\{R_0-|\delta R|, T_0\}$ lies to the left of the shifted stability boundary. So, an increase in diffusivity is stabilizing as before. It is difficult to prove, however, and we merely illustrate this in figure 8(*c*) with two examples.

In the analysis and examples shown in figures 7 and 8, we took starting points on the stability boundary. However, as should be clear from the graphs, generally, an increase in viscosity or diffusivity can be destabilizing too for initial points slightly left of the stability boundary, i.e. $\{R_0, T_0\}$ in the stable region.

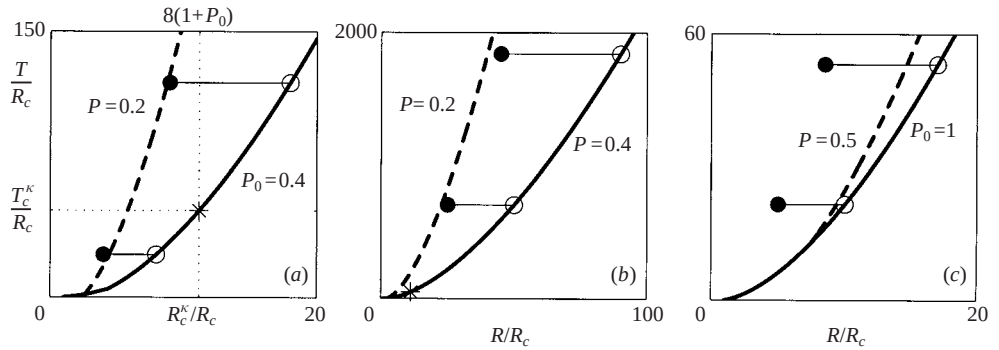

FIGURE 8. Graphs illustrating the stabilizing/destabilizing influence of increasing diffusivity. Initial points $\{R_0, T_0\}$ for some initial diffusivity κ_0 are marked by ○. In each case, κ is increased to $2\kappa_0$ and the final position of $\{R, T\}$ is marked by ●. (*a*) When $P < P_c$, an increase in diffusivity is stabilizing for points initially on the overstability section of the marginal stability boundary when below the critical point $\{R_c^\kappa, T_c^\kappa\}$ (marked by ∗), but destabilizing when above it. The example is for $P_0 = 0.4$. After doubling κ to $2\kappa_0$, the new stability boundary (dashed line) is defined by the final Prandtl number $P = 0.2$. (*b*) is as (*a*) but for points initially with larger R and T. For points initially on the convection curve section of the stability boundary, an increase in κ is stabilizing. (c) This is illustrated with an example where initially $P_0 = 1$. The dashed line indicates the final stability boundary defined by $P = 0.5$.

An increase in rotation (Ω) is always stabilizing because T increases. A decrease of the temperature gradient β is stabilizing as in non-rotating systems since it decreases R. A decrease in d affects both R and T, but it is still straightforward to show that the result is always stabilizing, as in non-rotating systems. This is true whether we consider decreasing d either with the temperature gradient β held fixed, or with the temperatures at the bottom and at the top held fixed.

4. Summary and discussion

We have revisited the classical linear stability problem for Rayleigh–Bénard convection in a rotating system with so-called 'free-free' rigid boundaries. In §2.1.1–§2.1.3, we discussed the properties of the cubic (2.1) which determines the stability boundaries in the space spanned by the Rayleigh, Taylor and Prandtl numbers. Because the coefficient B in (2.1) is always positive, we showed that stability/instability is entirely determined by the signs of D and $BC - D$, as summarized in table 1. Chandrasekhar sought to describe the convection curve and overstability curve in the RT-plane as curves $R_c^{(c)}(T)$ and $R_c^{(o)}(T, P)$, respectively. The critical wavenumbers for convection and overstability, $a_c^{(c)}(T)$ and $a_c^{(o)}(T, P)$, and the oscillation frequency of the overstable modes $\omega(T, P)$ were also calculated by him. In each case, he took the Taylor number as the independent variable. No closed-form formulae for the curves defining the marginal stability boundary were noted by him nor any for the critical wavenumbers, the frequency or the intersection point of the convection curve with the overstability curve. By switching to the Rayleigh number R as the independent variable, we have found in §§2.2.1 and 2.2.2 rather simple expressions for the convection curve $T_c^{(c)}(R)$ (2.19) and the overstability curve $T_c^{(o)}(R, P)$ (2.22). Similarly, the critical horizontal wavenumber for the onset of stationary convection $a_c^{(c)}(R)$ (2.20) and oscillatory convection $a_c^{(o)}(R, P)$ (2.23) are described by simple formulae, as well as the frequency

$\omega(R, P)$ (2.27) of the oscillations. None of these simple expressions appears to have been noted before. They enabled us to derive the exact expression for the point $\{R_i, T_i\}$ (2.25) beyond which the overstability curve determines the stability boundary and in § 3 the critical points $\{R_c^v, T_c^v\}$ (3.6) and $\{R_c^\kappa, T_c^\kappa\}$ (3.11) on the stability boundary beyond which an increase in viscosity or diffusivity destabilizes marginally stable systems.

When the Taylor number is used as the independent variable, all the critical numbers can also be expressed with closed-form formulae. For example, a cubic equation in R describing the convection curve follows with (2.19)

$$R^3 - R_c R^2 - 2R_c T R - R_c T^2 = 0. \tag{4.1}$$

Using the identity $4\cosh^3(z) - 3\cosh(z) = \cosh(3z)$ after a simple substitution which deletes the quadratic term $R_c R^2$, the convection curve $R_c^{(c)}(T)$ turns out to be described by

$$R_c^{(c)}(T) = R_c\left\{\frac{1}{3} + \frac{2}{3}(1 + 6(T/R_c))^{1/2}\cosh\left[\frac{1}{3}\operatorname{arcosh}\left(\frac{2 + 18(T/R_c) + 27(T/R_c)^2}{2(1 + 6(T/R_c))^{3/2}}\right)\right]\right\}. \tag{4.2}$$

The expression for the overstability curve $R_c^{(o)}(T, P)$ follows from (4.2) by replacing R and T with $R/(2+2P)$ and $P^2T/(1+P)^2$, respectively, as noted in § 2.2.2. Clearly, we would be hard-pressed to find the intersection point (2.25) by equating the expressions for $R_c^{(c)}(T)$ and $R_c^{(o)}(T, P)$. Similarly, (2.15) can be solved exactly to obtain the critical wavenumber for stationary convection as a function of the Taylor number. For $n = 1$, we find

$$a_c^{(c)}(T) = \pi\left\{\cosh\left[\frac{1}{3}\operatorname{arcosh}\left(1 + \frac{2T}{\pi^4}\right)\right] - \frac{1}{2}\right\}^{1/2}. \tag{4.3}$$

This may be compared to the inverse relation $a_c^{(c)}(R)$ given by (2.20). The critical wavenumber $a_c^{(o)}(T, P)$ for oscillatory convection follows by replacing T in (4.3) by $P^2T/(1+P)^2$. If the resulting (complicated) expression is substituted in (2.28), i.e. setting $a = a_c^{(o)}(T, P)$ in (2.28), we obtain a closed-form formula for the frequency of the oscillations $\omega(T, P)$ instead of (2.27) which determines ω along the overstability section of the stability boundary as a function of R and P. Obviously, (2.27) is much simpler. We believe that these far more complicated closed-form formulae are also new. In the literature, we found one example where such a closed-form formula is given (an expression for $a_c^{(c)}(T)$ by Kloeden & Wells 1983), but inspection showed that it was incorrect.

Chandrasekhar (1961, § 24) stated that 'in contrast to non-rotating fluids, an inviscid fluid in rotation should be expected to be thermally stable for *all* adverse temperature gradients. Indeed, only in the presence of viscosity can thermal instability arise', but this is wrong because as we have shown in § 2.3 the inviscid system is always unstable. Chandrasekhar (1961, § 32) treated R and T in this limit as numbers that remain finite, while the Prandtl number $P = \nu/\kappa$ tends to zero. The problem is that the time scale d^2/ν and the Rayleigh and Taylor number become indeterminate in the limit $\nu \to 0$. In his review of Chandrasekhar, Howard (1962) already voiced some doubts.

Finally, we point out the analogy between the present problem and that of an electrically conducting fluid subjected to a vertical magnetic field with the Lorentz forces replacing the Coriolis forces (Chandrasekhar 1961, chap. IV). Equally simple expressions for the marginal stability boundary, critical wavenumbers and

the frequency of overstable oscillations can be established when rigid stress-free boundaries are assumed.

This work has been supported by Office of Naval Research grants N00014-97-1-0095 and N00014-96-1-0762 and National Science Foundation grants OCE 97-30843, OCE 01-28991 and OCE 01-29301.

REFERENCES

Bénard, H. 1900 Les tourbillons cellulaires dans une nappe liquide. *Rev. Gén. Sci. Pur. Appl.* **11**, 1261–1271, 1309–1328.

Chandrasekhar, S. 1953 The instability of a layer of fluid heated below and subject to Coriolis forces. *Proc. R. Soc.* A **217**, 306–417.

Chandrasekhar, S. 1961 *Hydrodynamic and Hydromagnetic Stability*. Oxford University Press.

Chandrasekhar, S. & Elbert, D. D. 1955 The instability of a layer of fluid heated below and subject to Coriolis forces. II *Proc. R. Soc. Lond.* A **231**, 198–210.

Drazin, P. G. & Reid, W. H. 1981 *Hydrodynamic Stability*. Cambridge University Press.

Howard, L. N. 1962 Review of *Hydrodynamic and Hydromagnetic Stability* by S. Chandrasekhar. *J. Fluid Mech.* **12**, 158–160.

Kloeden, P. & Wells, R. 1983 An explicit example of Hopf bifurcation in fluid mechanics. *Proc. R. Soc. Lond.* A **390**, 293–320.

Manneville, P. 1990 *Dissipative Structures and Weak Turbulence*. Academic.

Rayleigh, Lord 1916 On convection currents in a horizontal layer of fluid when the higher temperature is on the under side. *Phil. Mag.* **32**, 529–546.

Rumford, Count 1797 The propagation of heat in fluids. In *The Collected Works of Count Rumford*, vol. 1 (ed. S. C. Brown). Harvard University Press, 1968.

Thomson, J. 1882 On a changing tesselated structure in certain liquids. *Proc. Phil. Soc. Glasgow* **13**, 464–468.